THE

PHYSICAL REVIEW

Millimeter-Wave Molecular-Beam Spectroscopy: Alkali Fluorides*

S. E. VEAZEY† AND WALTER GORDY

Department of Physics, Duke University, Durham, North Carolina

(Received 14 January 1965)

Rotational transitions of the alkali metal fluorides CsF, $Rb^{87}F$, $Rb^{85}F$, $K^{39}F$, NaF, and Li^7F have been measured in the millimeter- and submillimeter-wave regions where no previous measurements existed. The work was accomplished with a high-resolution molecular-beam absorption spectrometer, previously utilized for study of the other alkali halides. A more reliable oven was constructed and used to vaporize the alkali fluorides at temperatures up to 1100°C. Measurements on rotational transitions as high as $J = 27 \rightarrow 28$ in the first three vibrational states gave Y_{01}, Y_{11}, and Y_{21} more accurately, for the most part, than they were previously known, and gave Y_{02} and Y_{12} for the first time. From these Dunham rotational constants were derived potential coefficients, moments of inertia, internuclear distances, and vibrational constants.

INTRODUCTION

IN previous reports from this laboratory, measurements of millimeter-wave rotational spectra of the alkali bromides and iodides[1] and, more recently, of the alkali chlorides[2] have been described. These measurements were made with a molecular-beam absorption spectrometer[3] which greatly reduced Doppler broadening and collision broadening and which allowed exceptionally high-resolution and high-precision measurements to be made at the elevated temperatures required for vaporization of the alkali halides.

Because of their higher vaporization temperature, their greater chemical activity, and their greater tendency to form dimers in the vapor state, the fluorides have proved to be the most difficult of the halides for study in the microwave region. Honig *et al.*,[4] who obtained centimeter-wave data on most of the other halides with their hot-cell spectrometer, reported data for only one fluoride CsF, and that for only one transition, $J = 1 \rightarrow 2$. The molecular-beam-resonance method has been used for precise measurements of the $J = 0 \rightarrow 1$ transitions of RbF, KF, NaF, and Li^6F.

This method, however, is not applicable to higher J transitions because of the decreasing sensitivity of the Stark effect with increasing J. Because all the rotational constants are dependent to some extent on the centrifugal distortion effects, a complete solution for the rotational constants is not possible without measurements of the high J transitions which occur in the millimeter-wave region.

A re-design of the oven and an improvement in the sensitivity of the molecular-beam-absorption spectrometer have made possible high-precision measurements on all the alkali fluorides and an evaluation of all, or most of, the important rotational and vibrational constants of these molecules.

EXPERIMENTAL DETAILS

Except for the oven, the spectrometer design and the measuring procedure are essentially those described in the previous papers of this series.[1-3] At the temperatures required for observation of the fluorides, in the region of 1000°F, many failures were experienced with the wire heating coils used in the ovens of the previous experiments. Consequently, a new, hollow-tube oven made of thin stainless-steel tubing was designed and was found to operate successfully for all the fluorides. A sketch of this oven is shown in Fig. 1. The arrangement of the oven and the cell is shown in Fig. 2. The oven is a modification of the hollow-tube oven used in molecular-beam-resonance experiments, and the authors are indebted to Dr. W. Klemperer for giving them descriptive details. The hollow-tube oven is heated by

1 J. R. Rusk and W. Gordy, Phys. Rev. 127, 817 (1962).
2 P. L. Clouser and W. Gordy, Phys. Rev. 134, A863 (1964).
3 A. K. Garrison and W. Gordy, Phys. Rev. 108, 889 (1957).
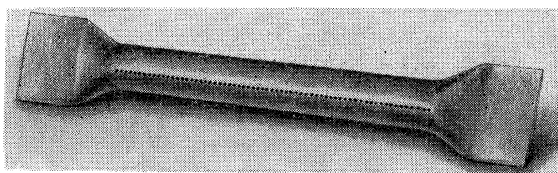4 A. Honig, M. Mandel, M. L. Stitch, and C. H. Townes, Phys. Rev. 96, 629 (1954).

FIG. 1. Sketch of oven.

TABLE I. Oven temperature required to vaporize alkali fluorides.

Alkali fluoride	Oven temperature in °C
CsF	650
RbF	720
KF	800
NaF	980
LiF	950

passage of a high current, up to 350 A, through the stainless steel tubing containing the salt sample. The tube is 11 in. long and is of either 1-in. o.d. and 0.010-in. wall thickness or $1\frac{1}{4}$-in. o.d. and 0.012-in. wall thickness. The former achieves temperatures up to a maximum of 1100°C. The latter reaches about 800°C. For salts which vaporize below 800°C, the larger tube is used as it holds a larger sample and thereby permits longer periods of vapor generation.

The oven tube has a 6-in. row of closely spaced holes, $\frac{1}{16}$ in. in diameter, drilled along the middle section of the tube for effusion of the salt. Although these holes do not form a well-collimated beam of salt, linewidths of 150 to 300 kc/sec are realized with an arrangement of baffles. The tube is crimped flat one inch from the end, loaded with salt, then crimped at the other end. The removable bottom of the vacuum chamber box serves as a base plate for the oven. The tube is clamped at each end by brass blocks which are supported by a pair of $\frac{5}{16}$-in. copper pipes. The pair of copper pipes at each end carry water to cool the blocks as well as the current to heat the stainless steel tube. The copper pipes penetrate the base plate through epoxy-resin insulators. There are four stainless-steel radiation shields which surround the oven tube. They are separated from the tube and from each other by lavite and alumina ceramic spacers. A water-cooled copper box with a stainless-steel top completely surrounds the radiation shields except for an opening to permit efflux of the salt.

A chromel-alumel thermocouple is used for measurement of oven temperature. It is insulated by alumina ceramic thermocouple insulating tubes from the Carborundum Company. The thermocouple measures the temperature at the outside surface near the center of the oven tube. Control of the current through the oven was afforded by two gauged variable autotransformers (type 136-2p from Superior Electric Company). The voltage from the autotransformer, which ranged up to 220 V, was fed into a step-down transformer and reduced to about 5 V.

Table I gives the approximate temperatures required to vaporize detectable amounts of the various alkali fluorides. These values varied slightly with different placement of the thermocouple. Accurate measurement of temperature was not required, but it was helpful to know at what temperature to expect generation of sufficient pressure for detection of transitions. These temperatures were recorded at the onset of vapor generation. However, temperatures were raised as much as 100°C to strengthen weak lines.

There are factors peculiar to particular alkali fluoride molecules which serve to reduce the absorption signal. The first of these is a division into isotopic species which simply reduces the number of molecules available for the transitions of a given species. Secondly, for some alkali fluorides a four-atom dimer molecule can exist as well as the diatomic molecule. This formation of dimers appears to be greater for the lighter alkali fluorides, as is evidenced by the weak lines observed in sodium fluoride and the yet weaker lines observed in lithium fluoride. Eisenstadt, Rothberg, and Kusch[5] studied the dissociation energies of the LiF, NaF, KF, RbF, and CsF dimers and found them to be 58.9, 54.3, 47.6, 42.0, and 37.8 kcal/mole, respectively. They also observed a lithium fluoride trimer and noted that the abundance of the dimer increases in the sequence CsF to LiF. There are other experimental evidences for large concentrations of dimers in lithium fluoride in particular and in the lithium halides in general.[6,7]

Table II gives the fraction of monomers for the different species, as determined by Schoonmaker and Porter.[6] It also gives the calculated fraction of molecules in the various observed vibrational states and that of molecules in the lower rotational state for the transition nearest to 200 kMc/sec. These fractions give an indication of the relative difficulties encountered in observation of the spectra. The most difficult spectra to observe were those of Li^7F. The spectra of Li^6F,
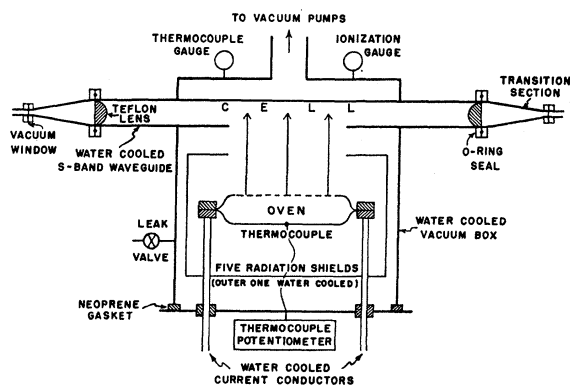

FIG. 2. Diagram of absorption cell and oven.

[5] M. Eisenstadt, G. M. Rothberg, and P. Kusch, J. Chem. Phys. 29, 797 (1958).

[6] R. C. Schoonmaker and R. F. Porter, J. Chem. Phys. 30, 283 (1959).

[7] J. Berkowitz, J. Chem. Phys. 29, 1386 (1958).

TABLE II. Fraction of observable molecules.

Molecule	F_J Rotational-state fraction or transition nearest 200 Gc/sec	F_v Vibrational-state fraction				Isotopic percentage	Monomer fraction[a]
		$v=0$	$v=1$	$v=2$	$v=3$		
CsF	0.0093	0.44	0.25	0.14	0.08	100.	0.77
Rb^{87}F	0.0085	0.42	0.24	0.14	0.08	27.8	0.63
Rb^{85}F	0.0085	0.42	0.24	0.14	0.08	72.2	0.63
K^{39}F	0.0077	0.39	0.24	0.14	0.09	93.1	0.51
NaF	0.0067	0.43	0.25	0.14	0.08	100.	0.55
Li^{7}F	0.0051	0.67	0.21	0.07	0.02	92.6	0.22

[a] Calculated from the data of Schoonmaker and Porter, Ref. 6.

abundance 7.4%, could not be detected, and the isotopic species K^{41}F (6.9%) was not considered.

THEORETICAL CONSIDERATIONS

The time-independent Schrödinger wave equation for a nonrigid rotor of masses m_1 and m_2 may be written in spherical coordinates as

$$\frac{h^2}{8\pi^2\mu r^2}\left[\frac{\partial}{\partial r}\left(r^2\frac{\partial\psi}{\partial r}\right)+\frac{1}{\sin\theta}\frac{\partial}{\partial\theta}\left(\sin\theta\frac{\partial\psi}{\partial\theta}\right)+\frac{1}{\sin^2\theta}\frac{\partial^2\psi}{\partial\phi^2}\right]$$
$$+V(r)\psi=E\psi, \quad (1)$$

where μ is the reduced mass $(m_1m_2)/(m_1+m_2)$ and where h is Planck's constant. Pekeris[8] has solved this equation for the allowed energies with $V(r)$ taken to be the Morse[9] potential:

$$V(r)=D[1-e^{-a(r-r_e)}]^2. \quad (2)$$

In this potential, D is the dissociation energy, r_e is the equilibrium internuclear distance, and a is a constant to be determined. The resulting energies[10] to the number of terms necessary to analyze the present data are expressed by

$$E_{Jv}/h=\omega_e(v+\tfrac{1}{2})-\omega_ex_e(v+\tfrac{1}{2})^2+B_vJ(J+1)$$
$$-D_vJ^2(J+1)^2+H_vJ^3(J+1)^3+\cdots, \quad (3)$$

where

$$B_v=B_e-\alpha_e(v+\tfrac{1}{2})+\gamma_e(v+\tfrac{1}{2})^2+\cdots, \quad (4)$$

$$D_v=D_e+\beta_e(v+\tfrac{1}{2})+\cdots, \quad (5)$$

and H_v may be approximated by

$$H_v\sim H_e=-(2D_e/3\omega_e^2)(12B_e^2-\alpha_e\omega_e). \quad (6)$$

Here ω_e is the vibrational frequency and ω_ex_e is the anharmonic correction constant. The term $B_e=h/8\pi^2I_e$ is corrected for vibration by the α_e and γ_e terms to form B_v. Similarly, D_e is the centrifugal stretching term; and vibrational interaction necessitates the correction term β_e.

A more accurate treatment is given by Dunham,[11]

who expanded the potential function about the equilibrium internuclear distance r_e in a power series of the form:

$$V(\xi)=ha_0c\xi^2(1+a_1\xi+a_2\xi^2+a_3\xi^3+\cdots), \quad (7)$$

where $\xi=(r-r_e)/r_e$. Dunham used the Wentzel-Kramers-Brillouin method to get the eigenvalues of Schrödinger's equation.[12] The energy equation so obtained may be written in the following form:

$$\frac{E_{J,v}}{h}=\sum_{lm}Y_{lm}(v+\tfrac{1}{2})^lJ^m(J+1)^m, \quad (8)$$

which when expanded reads

$$E_{J,v}/h=Y_{10}(v+\tfrac{1}{2})+Y_{20}(v+\tfrac{1}{2})^2+Y_{01}J(J+1)$$
$$+Y_{11}(v+\tfrac{1}{2})J(J+1)+Y_{12}(v+\tfrac{1}{2})J^2(J+1)^2$$
$$+Y_{02}J^2(J+1)^2+Y_{21}(v+\tfrac{1}{2})^2J(J+1)$$
$$+Y_{03}J^3(J+1)^3+\cdots. \quad (9)$$

When one applies the rotational absorption selection rules $\Delta J=+1$, $\Delta v=0$ to Bohr's postulate, one obtains a transition frequency of

$$\nu=(E_{J+1,v}-E_{J,v})/h$$
$$=2Y_{01}(J+1)+2Y_{11}(v+\tfrac{1}{2})(J+1)$$
$$+2Y_{21}(v+\tfrac{1}{2})^2(J+1)+4Y_{02}(J+1)^3$$
$$+4Y_{12}(v+\tfrac{1}{2})(J+1)^3+Y_{03}(J+1)^3$$
$$\times[(J+2)^3-J^3]+\cdots. \quad (10)$$

From comparison of Eqs. (3), (4), (5), with (9), it is seen that the following relations hold to first order:

$$\begin{array}{ll}
Y_{10}\sim\omega_e & Y_{20}\sim-\omega_ex_e \\
Y_{01}\sim B_e & Y_{11}\sim-\alpha_e \\
Y_{02}\sim-D_e & Y_{21}\sim\gamma_e \\
Y_{03}\sim H_e & Y_{12}\sim-\beta_e.
\end{array} \quad (11)$$

These approximations are adequate for our measurements except for Y_{01}, for which the accuracy of microwave measurements warrants the more accurate relation:

$$Y_{01}=B_e(1+B_e^2\beta_{01}/\omega_e^2), \quad (12)$$

[8] C. L. Pekeris, Phys. Rev. 45, 98 (1934).
[9] P. M. Morse, Phys. Rev. 34, 57 (1929).
[10] G. Herzberg, Molecular Spectra and Molecular Structure (D. Van Nostrand Company, Inc., New York, 1950), Vol. I.
[11] J. L. Dunham, Phys. Rev. 41, 721 (1932).
[12] J. L. Dunham, Phys. Rev. 41, 713 (1932).

where

$$\beta_{01} = (Y_{10}{}^2 Y_{21}/4 Y_{01}{}^3) + (16 a_1 Y_{20}/3 Y_{01}) \\ - 8a_1 - 6a_1{}^2 + 4a_1{}^3, \quad (13)$$

and where a_1 is given by Eq. (24).[11,13]

Some of the Y's which will be necessary for the data analysis are repeated from Dunham's paper for convenience (terms negligible for present purposes have been dropped):

$$Y_{00} = (B_e/8)(3a_2 - (7/4)a_1{}^2), \quad (14)$$

$$Y_{10} = \omega_e(1 + \cdots), \quad (15)$$

$$Y_{20} = B_e/2[3(a_2 - 5a_1{}^2/4) + \cdots], \quad (16)$$

$$Y_{01} = B_e[1 + (B_e{}^2/\omega_e{}^2)(15 + 14a_1 - 9a_2 + 15a_3 \\ - 23a_1a_2 + 21(a_1{}^2 + a_1{}^3)/2)], \quad (17)$$

$$Y_{11} = B_e{}^2/\omega_e[6(1 + a_1) + \cdots], \quad (18)$$

$$Y_{21} = (6B_e{}^3/\omega_e{}^2)[5 + 10a_1 - 3a_2 + 5a_3 - 13a_1a_2 \\ + 15(a_1{}^2 + a_1{}^3)/2], \quad (19)$$

$$Y_{02} = -(4B_e{}^3/\omega_e{}^2)[1 + \cdots], \quad (20)$$

$$Y_{12} = -(12B_e{}^4/\omega_e{}^3)(19/2 + 9a_1 + 9a_1{}^2/2 - 4a_2), \quad (21)$$

$$Y_{03} = 16B_e{}^5(3 + a_1)/\omega_e{}^4, \quad (22)$$

$$a_0 = (\omega_e{}^2/4B_e)c, \quad (23)$$

$$a_1 = (Y_{11}Y_{10}/6Y_{01}{}^2) - 1. \quad (24)$$

Now, solving Eqs. (21), (19), and (20), respectively, one gets

$$a_2 = Y_{12}\omega_e{}^3/48B_e{}^4 + 19/8 + 9/4a_1 + 9/8a_1{}^2, \quad (25)$$

$$a_3 = \omega_e{}^2 Y_{21}/30B_e{}^3 - 1 - 2a_1 + 3/5a_2 + 13/5a_1a_2 \\ - 3/2(a_1{}^2 + a_1{}^3), \quad (26)$$

and

$$\omega_e = 2(B_e{}^3/Y_{02})^{1/2}. \quad (27)$$

From the definition of B_e, one finds that

$$I_e = h/8\pi^2 B_e = 505587.4/B_e \text{ amu Å}^2, \quad (28)$$

where B_e is expressed in Mc/sec,[14] and $\hbar = h/2\pi = 1.05443 \pm 0.00004 \times 10^{-27}$ erg-sec.[15] From I_e, the term r_e may be calculated from the equation

$$r_e = (I_e/\mu)^{1/2} \text{ Å}, \quad (29)$$

where the reduced mass μ is in amu.

One can often obtain formulas in more common nomenclature by substitution of the potential coefficients. Herzberg[10] gives the useful formula:

$$\beta_e = D_e \frac{8\omega_e x_e}{e} - \frac{5\alpha_e}{B_e} - \frac{\alpha_e{}^2 \omega_e}{24B_e{}^3}, \quad (30)$$

by which $\omega_e x_e$ may be calculated. He also lists another important formula shown by Pekeris to be valid for the Morse potential:

$$\alpha_e = 6((\omega_e x_e B_e{}^3)^{1/2}/\omega_e) - 6B_e{}^2/\omega_e. \quad (31)$$

The use of some equations will be amplified in the following material.

The rotational transitions measured in this study involve such high-J values that the nuclear hyperfine structure is not resolvable. Hence the theory of hyperfine structure in rotational spectra is not required here.

ANALYSIS OF DATA

The major data analysis was accomplished on the IBM-7072 digital computer in the Duke University Digital Computing Laboratory. First an auxiliary program was used to calculate the expected line frequencies according to Eq. (10) without, however, the small term in Y_{03}. Previous data comprising Y_{01}, Y_{11}, and Y_{21} were used. Theoretical estimates according to Eq. (21) were used for Y_{02}. Once a solution for the Y_{lm}'s was made, these new values (now including Y_{12}) were inserted into the program the better to pinpoint lines for future measurement. The program computed all J transitions in the first four vibrational states within the measurement capabilities of the spectrometer. In addition, the program output gave the quantum numbers, the klystron frequencies, the harmonics, and the expected receiver readings. This program was valuable in that it saved many hours at the desk calculator and made assignment of quantum numbers to a measurement a simple task.

A second program calculated the fraction of molecules in each vibrational state and each rotational state, also the absorption coefficient for each transition. This served as an aid in the determination of the transitions for which to search and in the estimate of the sensitivity necessary for detection of these transitions.

The majority of the data reduction was done with computer programs written and described by Clouser.[16] Before the measured frequencies ν_i were processed, they were corrected by subtraction of the last term in Eq. (10), which is quite small. The Y_{03} or H_e constant is approximated by Eq. (6) and the coefficient $(J+1)^3 \times [(J+2)^3 - J^3]$ is taken from an output table of these values prepared by the computer. The n ($n \geq 5$) corrected frequencies ν_i' appear in the form

$$\nu_i' = \nu_i - (J+1)^3 [(J+2)^3 - J^3] Y_{03} \\ = 2(J+1)Y_{01} + 2(J+1)(v+\tfrac{1}{2})Y_{11} \\ + 2(J+1)(v+\tfrac{1}{2})^2 Y_{21} + 4(J+1)^3 Y_{02} \\ + 4(J+1)^3(v+\tfrac{1}{2})Y_{12}. \quad (32)$$

These n equations are reduced to five normal equations in the five unknown Y_{lm}'s. These normal equations are

[13] C. H. Townes and A. L. Schawlow, *Microwave Spectroscopy* (McGraw-Hill Book Company, Inc., New York, 1955).

[14] W. Gordy, W. V. Smith, and R. F. Trambarulo, *Microwave Spectroscopy* (John Wiley & Sons, Inc., New York, 1953).

[15] J. W. Dumond and E. R. Cohen, *Handbook of Physics*, edited by E. U. Condon and H. Odishaw (McGraw-Hill Book Company, Inc., New York, 1958), p. 7-143.

[16] P. L. Clouser, Ph.D. thesis, Duke University, 1963 (unpublished).

TABLE III. Transition frequencies of CsF.

J	v	Measured frequency (Mc/sec)	Calculated frequency (Mc/sec)	Difference (Mc/sec)
8	0	99 156.072	99 156.071	−0.001
9	0	110 168.823	110 168.814	−0.009
12	0	143 197.757	143 197.748	−0.009
15	0	176 209.640	176 209.690	+0.050
16	0	187 209.275	187 209.217	−0.058
18	0	209 200.722	209 200.720	−0.002
19	0	220 192.344	220 192.404	+0.060
20	0	231 181.206	231 181.185	−0.021
27	0	308 009.125	308 009.116	−0.009
8	1	98 522.943	98 522.952	+0.009
9	1	109 465.332	109 465.341	+0.009
12	1	142 283.228	142 283.200	−0.028
16	1	186 013.250	186 013.193	−0.057
20	1	229 703.592	229 703.625	+0.033
8	2	97 891.179	97 891.197	+0.018
9	2	108 763.371	108 763.384	+0.013
12	2	141 370.596	141 370.622	+0.026
16	2	184 819.760	184 819.746	−0.014
8	3	97 260.822	97 260.806	−0.016

TABLE IV. Transition frequencies of $Rb^{87}F$.

J	v	Measured frequency (Mc/sec)	Calculated frequency (Mc/sec)	Difference (Mc/sec)
8	0	112 771.005	112 771.000	−0.005
13	0	175 370.290	175 370.338	+0.048
14	0	187 882.995	187 882.953	−0.042
15	0	200 392.716	200 392.703	−0.013
17	0	225 402.840	225 402.851	+0.011
8	1	111 958.326	111 958.324	−0.002
14	1	186 528.030	186 528.031	+0.001
17	1	223 776.564	223 776.563	−0.001
14	2	185 179.055	185 179.054	−0.001

constructed to minimize the errors squared and summed. These five equations are then solved for the Y_{lm}'s.

The error limits of the standard frequency markers employed are less than 0.004 Mc/sec at the highest measured frequencies. This is well within the dispersion of the meter readings, and hence the over-all accuracy is limited by the ability of the experimenter to visually align the marker and the transition's "pip" on the oscilloscope. These random human errors may be treated statistically.

The errors of each Y_{lm} are computed in the manner described by Topping.[17] First the difference d_i between the measured frequencies and the calculated frequencies computed from the new Y_{lm}'s is obtained. Then the standard error α of the frequencies is defined by

$$\alpha = \sum_i d_i^2 / (n-5), \qquad (33)$$

where 5 is the number of unknowns. As many lines as practical are measured to increase n and hence reduce

---

[17] J. Topping, Errors of Observation and Their Treatment (The Institute of Physics, London, 1956).

the standard error. Actually, each line is measured at least three times and in most cases more than three times. These three or more measurements are averaged and recorded as the measured line frequency. Finally the error for each Y_{lm} is described by the equation

$$\alpha_{lm} = [(\Delta_{lm}/\Delta)\alpha^2]^{1/2}, \qquad (34)$$

where Δ is the determinant of the coefficients and Δ_{lm} is the minor of the Y_{lm} in the set of normal equations.

The other spectral constants are calculated in a straightforward manner with the equation given above. In the process, an iteration procedure is used to achieve a better solution for B_e after Y_{01} is initially set equal to B_e in the parenthetical quantity of Eq. (12). Errors of the derived constants come from a first differential of the equation for the derived constant in terms of the measured constants and their errors.

OBSERVED SPECTRA AND ROTATIONAL CONSTANTS

In Tables III through VIII are recorded the measured frequencies. The five Y_{lm}'s (Y_{01}, Y_{11}, Y_{21}, Y_{02}, and Y_{12}) computed from these measured frequencies (corrected

TABLE V. Transition frequencies of $Rb^{85}F$.

J	v	Measured frequency (Mc/sec)	Calculated frequency (Mc/sec)	Difference (Mc/sec)
7	0	100 667.499	100 667.475	−0.024
8	0	113 246.036	113 245.988	−0.048
10	0	138 397.632	138 397.611	−0.021
14	0	188 673.835	188 673.836	+0.001
15	0	201 236.076	201 236.136	+0.060
17	0	226 351.230	226 351.280	+0.050
20	0	263 997.503	263 997.454	−0.049
23	0	301 607.144	301 607.141	−0.003
7	1	99 940.248	99 940.231	−0.017
8	1	112 427.805	112 427.846	+0.041
14	1	187 310.440	187 310.364	−0.076
15	1	199 781.736	199 781.788	+0.052
17	1	224 715.192	224 715.195	+0.003
14	2	185 952.825	185 952.724	−0.001

TABLE VI. Transition frequencies of KF.

J	v	Measured frequency (Mc/sec)	Calculated frequency (Mc/sec)	Difference (Mc/sec)
5	0	100 275.855	100 275.861	+0.006
6	0	116 983.272	116 983.230	−0.042
7	0	133 688.188	133 688.164	−0.024
8	0	150 390.286	150 390.317	+0.031
9	0	167 089.325	167 089.340	+0.015
10	0	183 784.847	183 784.884	+0.037
11	0	200 476.632	200 476.604	−0.028
13	0	233 847.180	233 847.173	−0.007
5	1	99 440.820	99 440.838	+0.018
6	1	116 009.004	116 009.039	+0.035
7	1	132 574.884	132 574.806	−0.078
9	1	165 697.625	165 697.651	+0.026
5	2	98 610.756	98 610.773	+0.017
6	2	115 040.649	115 040.633	−0.016

TABLE VII. Transition frequencies of NaF.

J	v	Measured frequency (Mc/sec)	Calculated frequency (Mc/sec)	Difference (Mc/sec)
3	0	104 229.592	104 229.599	+0.007
4	0	130 280.736	130 280.738	+0.002
5	0	156 327.692	156 327.701	+0.009
6	0	182 369.675	182 369.655	−0.020
9	0	260 457.106	260 457.109	+0.003
3	1	103 147.626	103 147.611	−0.015
4	1	128 928.204	128 928.256	+0.052
5	1	154 704.784	154 704.728	−0.056
6	1	180 476.177	180 476.195	+0.018
3	2	102 076.572	102 076.571	−0.001

TABLE VIII. Transition frequencies of Li^{7}F.

J	v	Measured frequency (Mc/sec)	Calculated frequency (Mc/sec)	Difference (Mc/sec)
1	0	160 096.288	160 096.287	−0.001
2	0	240 123.469	240 123.469	+0.000
1	1	157 701.445	157 701.445	+0.000
2	1	236 530.480	236 530.479	−0.001
1	2	155 346.420	155 346.419	−0.001

the ones used in a second iteration. The equation used to calculate the Y_{03} or H_e correction term is

$$Y_{03} = 2(D_e/3\omega_e^2)(12B_e - \alpha_e\omega_e), \qquad (35)$$

which may be derived from Eqs. (22) and (24). The correction to the line frequencies by the Y_{03} term multiplied by the appropriate coefficient is within the dispersion of the frequency measurements. There is usually no correction to low-J transition frequencies, and the higher J transition frequencies are corrected by only a few kilocycles.

The Y_{04} term in some cases has an error larger than the term itself, and its value is smaller by two orders of magnitude than Y_{03}. For this reason it was not considered in the frequency equation.

Cesium fluoride. Cesium fluoride is the heaviest of the molecules studied, and as such it has the most transitions within the range of the spectrometer. The 19 measured transitions for this molecule comprise the largest set of measurements, and this set includes the only measurement in the third vibrational state. Cesium has only one isotope, and cesium fluoride has the smallest dimer-to-monomer and trimer-to-monomer

TABLE IX. Comparison of measured rotational constants.

Molecule	Y_{01} (Mc/sec) Present	Y_{01} (Mc/sec) Previous	Y_{11} (Mc/sec) Present	Y_{11} (Mc/sec) Previous	Y_{21} (Mc/sec) Present	Y_{21} (Mc/sec) Previous	$-Y_{02}$ (kc/sec) Present[a]	Y_{12} (kc/sec) Present[a]
CsF	5 527.265 ±0.001	5 527.27[b] ±0.04	35.247 ±0.002	33.13[b] ±0.05	0.038 ±0.001	0.009[b] ±0.012	6.046 ±0.001	−0.009 ±0.002
Rb^{87}F	6 288.988 ±0.003	6 289.002[c] ±0.010	45.338 ±0.004	45.350[c] ±0.017	0.099 ±0.001	0.094[c] ±0.007	7.926 ±0.006	−0.054 ±0.006
Rb^{85}F	6 315.548 ±0.003	6 315.543[d] ±0.009	45.652 ±0.004	45.638[c] ±0.017	0.099 ±0.001	0.094[c] ±0.007	8.046 ±0.004	0.011 ±0.005
KF	8 392.313 ±0.005	8 392.309[e] ±0.004	69.999 ±0.008	69.991[d] ±0.010	0.207 ±0.002	0.204[d] ±0.005	14.493 ±0.016	0.007 ±0.025
NaF	13 097.951 ±0.007	13 097.971[f] ±0.003	136.618 ±0.014	136.665[f] ±0.005	0.684 ±0.004	0.700[f] ±0.001	34.797 ±0.045	0.021 ±0.072
Li^{7}F	40 329.907 ±0.150	40 329.987[g] ±0.005	608.569 ±0.250	608.154[g] +0.005	4.977 +0.030	4.633[g] +0.005	343. ±9.	12. ±4.

[a] There are no previously measured values for Y_{02} and Y_{12}.
[b] Honig *et al.*, Ref. 4.
[c] Lew *et al.*, Ref. 19.
[d] Green and Lew, Ref. 20.
[e] Ritchie and Lew, Ref. 22.
[f] Bauer and Lew, Ref. 21.
[g] Wharton *et al.*, Ref. 23 (mass ratio conversions of their Li^{6}F constants).

for the Y_{03} term) are listed in Table IX. These five constants are termed the measured rotational constants, whereas the other Y_{lm}'s and all of the other information in this section are derived from these measured Y_{lm}'s. To show the degree of consistency in the data, the frequencies calculated with the chosen Y_{lm} values are listed in Tables III–VIII for comparison with the observed ones.

The Y_{lm}'s which were not directly measured but which could be calculated with reasonable error limits appear in Table X. The Y_{13} value was calculated, but the error limits were greater than the value of the constant itself; therefore, it is not listed. The Y_{00} value represents a correction to the zero-point vibrational energy.

The Y_{03} values listed in Table X are unchanged from

ratios of any of the alkali fluorides. These factors combine to produce the most easily detectable and measurable transitions of this series. Figure 3 shows the oscilloscope photographs of the $J = 12 \rightarrow 13$ rota-

TABLE X. Calculated Dunham constants.

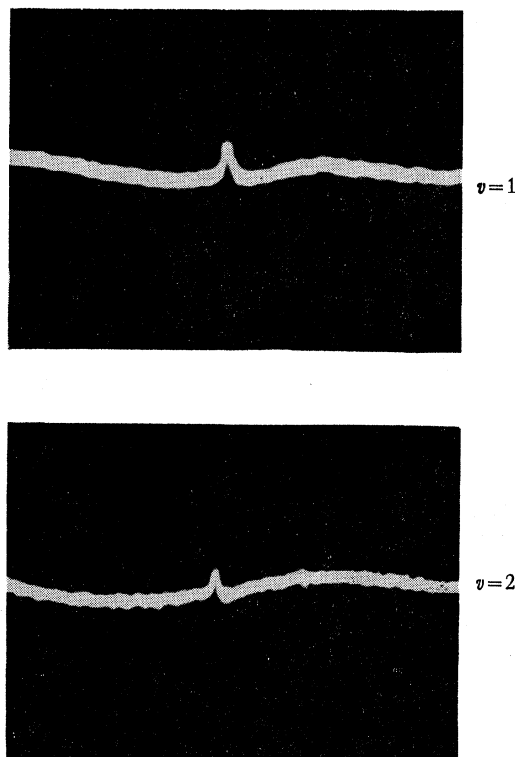| Molecule	Y_{00} (Gc/sec)	Y_{03} (cps×10^{-3})	Y_{04} (cps×10^{-3})
CsF	0.596 ±0.092	−0.214 ±0.002	−0.0054 ±0.0004
Rb^{85}F	2.021 ±0.249	−1.381 ±0.008	−0.0041 ±0.0016
KF	2.144 ±0.753	−2.895 ±0.042	−0.0197 ±0.0116
NaF	3.464 ±1.153	−12.306 ±0.179	−0.112 ±0.066
Li^{7}F	34. ±14.	807. ±110.	35. ±37.

FIG. 3. Oscilloscope tracing of the $J=12 \rightarrow 13$ rotational transition of CsF in excited vibrational states $v=1$ and $v=2$.

tional transitions in the two excited vibrational states. The $J=27 \rightarrow 28$ transition has the highest measured frequency, at 308 009.125 Mc/sec, which falls barely within the submillimeter wave region.

The five rotational structure constants derived from a solution of these nineteen measurements are given in Table IX (the J quantum number is the lower state of the transition). The Columbia University group measured the cesium fluoride transition $J=1 \rightarrow 2$ in the first five vibrational states.[4] However, the accuracy of their measurements is only one part in 10^4, whereas the present measurements are accurate to one part in 10^6. As a result, the values of Y_{01}, Y_{11}, and Y_{21} reported here are an order of magnitude more accurate than those obtained from their measurements (see Table IX). There is agreement within the stated errors on the Y_{01} term, but there is disagreement on the Y_{11} and Y_{21} terms. This discrepancy may have arisen because Honig et al., used Barrow and Caunt's[18] value of ω_e to estimate D_e. Similar discrepancies were noted in the comparisons of alkali bromide,[1] iodide,[1] and chloride[2] data from this spectrometer with those from the hot cell spectrometer of the Columbia group. For the alkali fluorides, Y_{02} and Y_{12} are here experimentally measured for the first time (Table IX).

Rubidium fluoride. Both isotopes of rubidium fluoride,

Rb⁸⁷F and Rb⁸⁵F, were measured. Their observed frequencies are listed in Tables IV and V, respectively. Because Rb⁸⁵F is approximately three times more abundant than Rb⁸⁷F, its spectral lines were stronger, and hence more of them were measured.

Lew et al.[19] have measured the Rb⁸⁵F, $J=0 \rightarrow 1$ transition in the $v=0$, 1, and 2 states by the molecular beam electric resonance method. They measured the Rb⁸⁷F, $J=0 \rightarrow 1$ transition only in the $v=0$ state. Their quoted errors on the measurements vary from 5 to 10 kc/sec at a frequency of about 12 Gc/sec. The present measurements have errors within, at most, 75 kc/sec, and averaging 30 kc/sec at frequencies from 100 to 300 Gc/sec. Consequently, the relative accuracy of our measurements is approximately twice that of the electric beam resonance measurements. The values of Y_{01}, Y_{11}, and Y_{21} gratifyingly agree to within the errors of both determinations (see Table IX). These constants, as determined by this experiment, show an improvement in error limit by a factor of about three.

Potassium fluoride. This salt gave the most experimental difficulty of the three deliquescent salts CsF, RbF, and KF. The first attempt to measure potassium fluoride was disappointing; hydrogen fluoride from the reaction $KF + H_2O \rightarrow KOH + HF$ etched the glass components and polluted the pump oil. Furthermore, the relatively insoluble KOH clogged the oven. Once these difficulties were solved by complete dehydration of the sample, 14 lines were measured in three vibrational states. The frequencies are listed in Table VI.

Green and Lew[20] measured KF by the molecular beam electric resonance method. The constants Y_{01}, Y_{11}, and Y_{21} as determined by their measurements agree very well with the present measurements (Table IX).

Sodium fluoride. Sodium fluoride was the most difficult of the salts to vaporize: an oven temperature of almost 1000°C was required. Because sodium fluoride is not hygroscopic, however, the cumbersome dry box operation could be bypassed. The transitions listed in Table VII were measured in three vibrational states. One transition is shown in Fig. 4.

Bauer and Lew[21] measured sodium fluoride by the molecular beam electric resonance method. At the beginning of their work no accurate value of ω_e for NaF existed. In order to estimate D_e to reduce their data, they needed a good value of ω_e. Consequently, in a separate experiment Ritchie and Lew[22] measured ω_e and $\omega_e x_e$ for NaF. Their value of ω_e, the best to date, agrees well within both our stated errors to the value determined from the D_e term measured by this experiment (see Table XI). The values of Y_{01}, Y_{11}, and Y_{21}

[18] R. F. Barrow and A. D. Caunt, Proc. Roy. Soc. (London) A219, 120 (1953).

[19] H. Lew, D. Morris, F. E. Geiger, Jr., and J. T. Eisinger, Can. J. Phys. 36, 171 (1958).
[20] G. W. Green and H. Lew, Can. J. Phys. 38, 482 (1960).
[21] R. K. Bauer and H. Lew, Can. J. Phys. 41, 1461 (1963).
[22] R. K. Ritchie and H. Lew, Can. J. Phys. 42, 43 (1964).

TABLE XI. Vibrational constants.

Molecule	Present ω_e (cm^{-1})	Previous values ω_e (cm^{-1})			Rittner's calculated[a] ω_e (cm^{-1})	Present $\omega_e x_e$ (cm^{-1})	Previous $\omega_e x_e$ (cm^{-1})	
CsF	352.56 ±0.04	357.[b] ±15.	385.[c]	270.[d] ±30.	345	−1.62 ±0.01	1.23[c]	
Rb[87]F	373.74 ±0.14	378.[b] ±10.				−2.18 ±0.03		
Rb[85]F	373.27 ±0.08	378.[b] ±10.	390.,[c]	340.[e] ±68.	361	−1.80 ±0.03	1.3[c]	
KF	426.04 ±0.24	429.,[b] ±3.	405.,[c]	390.[f] ±39.	410	−2.43 ±0.09	1.45,[c] ±0.25	2.4[b]
NaF	536.10 ±0.35	536.[b] ±2.			477	−3.83 ±0.14	3.4[b] ±0.25	
Li[7]F	922. ±12.	910.34,[g,h] ±32.	646.,[i] ±5.	897.[j]	773	−5.4 ±1.5	7.90,[h] ±0.01 ±0.5	7.3[j]
Li[6]F		964.07,[g]	756.,[i] ±38.	930.[k] ±19.			8.8953[g]	

a E. S. Rittner, J. Chem. Phys. 19, 1030 (1951).
b Ritchie and Lew (Ref. 22) (KF and NaF are measurements, RbF and CsF extrapolations).
c Barrow and Caunt, Ref. 18.
d J. W. Trischka, Phys. Rev. 76, 1365 (1949).
e V. Hughes and L. Grabner, Phys. Rev. 79, 314 (1950).

f L. Grabner and V. Hughes, Phys. Rev. 79, 819 (1950).
g Wharton et al., Ref. 23.
h Vidale, Ref. 24.
i R. Braunstein and J. W. Trischka, Phys. Rev. 98, 1092 (1955).
j Vasilevskii and Baikov, Ref. 25.
k T. I. Moran and J. W. Trischka, J. Chem. Phys. 34, 923 (1961).

(Table IX) are slightly outside the stated errors, however.

Lithium fluoride. Lithium fluoride has the two isotopes Li[7]F and Li[6]F, the first of which is much the more plentiful (abundance 92.6%). However, only the Li[6]F isotopic species had been studied previously with the electric beam resonance method. Wharton et al.,[23] chose isotopically pure Li[6]F over the more abundant Li[7]F because of the smallness of the Li[6] nuclear electric quadrupole interaction. This present study is the first microwave experiment on the Li[7]F molecule of which the authors are aware. Because of the large B_e value, there are only two J transitions within the range of this spectrometer. The data in Table II show the reason for the weakness of the microwave lines of LiF. Dimerization is very high, and the higher vibrational states are only lightly populated. Because the measurements
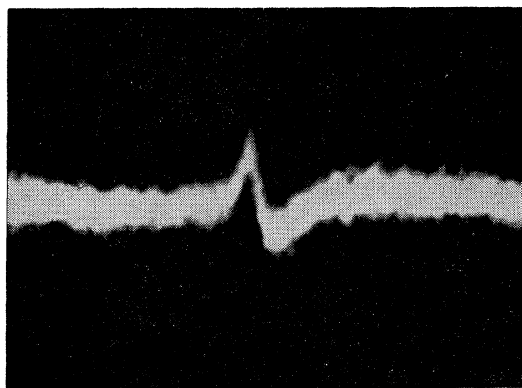

FIG. 4. Oscilloscope tracing of the $J = 5 \rightarrow 6$ rotational transition of NaF in the ground vibrational state. The line frequency is 156 327.7 Mc/sec and the linewidth is 200 kc/sec. The vapor temperature is approximately 1000°C.

[23] L. Wharton, W. Klemperer, L. P. Gold, R. Strauch, J. J. Gallagher, and V. E. Derr, J. Chem. Phys. 38, 1203 (1963).

were difficult and few transitions were observed, the spectral constants for LiF are not obtained with as great an accuracy as those for the other alkali fluorides.

VIBRATIONAL CONSTANTS

The vibrational constants ω_e and $\omega_e x_e$ are listed in Table XI with other values for comparison. The present values are calculated by Eqs. (20) and (30), respectively. All of the ω_e values agree with the latest and most accurate determinations of this vibrational constant. Except for Li[7]F, the values of ω_e from this experiment appear to be one of two orders of magnitude more accurate than those from infrared spectra.

Vidale[24] made some very accurate infrared measurements of Li[7]F. Unfortunately, because of an unresolved ambiquity in the assigned value of the J quantum number, he gave three sets of possible vibrational and rotational constants (Table XII). The present work

TABLE XII. Li[7]F comparison with Vidale's three sets of parameters.

Parameter	Present Li[7]F	Vidale's sets[a] (1)	(2)	(3)
ω_e(cm^{-1})	922.	904.85	907.64	910.34
$\omega_e x_e$(cm^{-1})	5.4	7.889	7.910	7.929
α_e(cm^{-1})	0.020299	0.019556	0.019856	0.020000
B_e(cm^{-1})	1.3454	1.3881	1.3676	1.3468
r_e(Å)	1.563904	1.5397	1.5512	1.5631

a Vidale, Ref. 24.

shows directly that the third set of Vidale's results (the one he considered much less probable) is the true one. Wharton et al.[23] indirectly inferred that Vidale's third set was the correct one by mass ratio conversion

[24] G. L. Vidale, J. Phys. Chem. 64, 314 (1960).

of their Li^6F data. Now Vidale's values of $\omega_e = 910.34$ cm^{-1} and $\omega_e x_e = 7.929$ cm^{-1} from set (3) should be considered the best values available for Li^7F.

The present calculations of $\omega_e x_e$ are consistently higher than the values for CsF, RbF, KF, and NaF of Barrow and Caunt[18] and Ritchie and Lew[22] (Table XI). The same kind of difference was found for alkali bromides and alkali iodides.[1] The present Li^7F $\omega_e x_e$ value is not as reliable as that of the other alkali fluorides. Although it lies below the values of Vidale[24] and of Vasilevskii and Baikov,[25] it agrees within experimental error with the value quoted by the latter.

POTENTIAL COEFFICIENTS

The potential coefficients a_0, a_1, a_2, and a_3 are calculated with equations given in theoretical considerations. These values are listed in Table XIII. In Eq. (23), ω_e

TABLE XIII. Dunham's potential coefficients.

Molecule	a_0 (cm$^{-1}\times10^{-5}$)	a_1	a_2	a_3
CsF	1.6855	−3.0324	5.65	−7.2
	±0.0003	±0.0003	±0.04	±0.4
Rb^{87}F	1.6646	−3.1406	5.40	−2.2
	±0.0013	+0.0010	±0.11	±1.1
Rb^{85}F	1.6535	−3.1347	6.58	−11.4
	±0.0007	±0.0007	±0.10	±1.0
KF	1.6210	−3.1157	6.34	−9.6
	±0.0018	±0.0014	±0.23	±2.2
NaF	1.6445	−3.1331	6.43	−9.2
	±0.0021	±0.0016	±0.23	±2.1
Li^{7}F	1.5802	−2.7239	6.60	−17.2
	±0.0414	±0.0233	±0.89	±8.3

is in cm^{-1}, B_e is in Mc/sec, and the value of c is taken to be 2.99793×10^{10} cm/sec.[15] Therefore the units of a_0 are cm^{-1}, while the remaining coefficients are dimensionless. There is substantial agreement with the summary of these coefficients based on previous data given by Ritchie and Lew[22] for all the alkali fluorides excluding lithium fluoride. The previous evaluations of the potential coefficients were seriously limited by inaccurate values of ω_e.

MOMENTS OF INERTIA AND INTERNUCLEAR DISTANCES

Table XIV gives the values of molecular constants B_e, β_{01}, I_e, and r_e. The B_e term is calculated by an iteration procedure according to Eq. (12); β_{01} comes from Eq. (13). Then I_e and r_e are obtained by Eqs. (28) and (29), respectively. The atomic masses used

[25] K. P. Vasilevskii and V. I. Baikov, Opt. i Spektroskopiya 11, 41 (1961) [English transl.: Opt. Spectry. (USSR) 11, 21 (1961)].

TABLE XIV. Molecular constants.

Molecule	B_e (Mc/sec)	β_{01}	I_e (amu-Å^2)	r_e (Å)
CsF	5527.266	−0.7	91.4715	2.345462
	±0.002	±1.0	±0.0035	±0.000045
Rb^{87}F	6288.957	16.1	80.3929	2.270450
	±0.007	±2.8	±0.0031	±0.000044
Rb^{85}F	6315.576	−14.2	80.0540	2.270435
	±0.006	±2.6	±0.0031	±0.000043
KF	8392.349	−10.0	60.2438	2.171554
	±0.009	±5.8	±0.0023	±0.000042
NaF	13 098.042	−10.5	38.6002	1.926032
	±0.014	±5.7	±0.0015	±0.000037
Li^{7}F	40 333.798	−45.3	12.5351	1.563861
	±0.300	±19.0	±0.0005	±0.000033

in the calculation of r_e are those given by Johnson, Quisenberry, and Nier.[26]

Table XV compares our r_e values with previously

TABLE XV. Comparison of internuclear distances.[a]

Molecule	Present r_e (Å)	Other r_e (Å)	Theoretical[b] value r_e (Å)
CsF	2.34546 (4)	2.3453 (1)[c]	2.345
Rb^{87}F	2.27045 (4)	2.27031 (5)[d]	2.259
Rb^{85}F	2.27043 (4)	2.27031 (5)[d]	2.259
KF	2.17155 (4)	2.17146 (5)[e]	2.166
NaF	1.92603 (4)	1.92595 (6)[f]	1.917
Li^{7}F	1.56386 (3)	1.563 (6)[g]	1.584
Li^{6}F		1.56389 (5)[h]	1.584

[a] The figures in parentheses indicate the uncertainty in the last digit.
[b] Green and Lew, Ref. 20.
[c] Honig et al., Ref. 4.
[d] H. Lew, National Research Council No. 7887, 1004, 1964 (unpublished) (a correction to the value given by H. Lew et al., Ref. 19).
[e] R. K. Ritchie and H. Lew, Ref. 22 (a correction to the value of G. W Green and H. Lew, Ref. 20).
[f] Bauer and Lew, Ref. 21.
[g] Vidale, Ref. 24.
[h] Wharton et al., Ref. 23.

measured ones. The rubidium fluoride values disagree slightly outside the quoted error limits. Vidale's best r_e value of 1.545 Å for Li^7F is known to be in error since he did not use the correct set of data to obtain it. The set now shown to be correct gives the value of 1.5631 Å, which is in excellent agreement with the present value. It will be noted that the internuclear distances of the rubidium and lithium isotopic species agree closely with each other.

ACKNOWLEDGMENTS

[26] H. Johnson, K. S. Quisenberry, and A. O. Nier, Handbook of Physics, edited by E. U. Condon and H. Odishaw (McGraw-Hill Book Company, Inc., New York, 1958), p. 9–55.
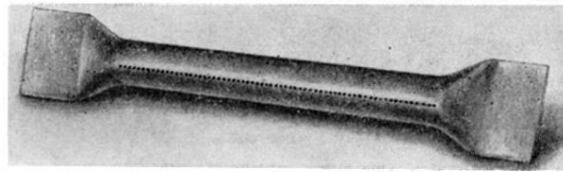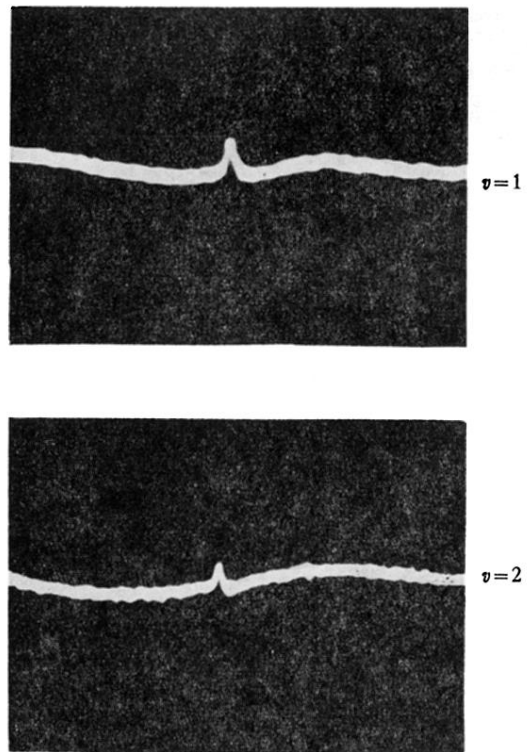
FIG. 1. Sketch of oven.

FIG. 3. Oscilloscope tracing of the $J = 12 \rightarrow 13$ rotational transition of CsF in excited vibrational states $v = 1$ and $v = 2$.
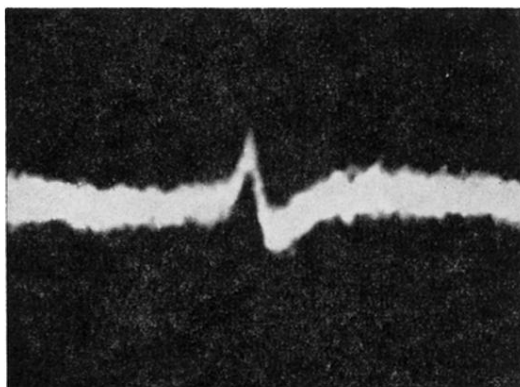
FIG. 4. Oscilloscope tracing of the $J = 5 \rightarrow 6$ rotational transition of NaF in the ground vibrational state. The line frequency is 156 327.7 Mc/sec and the linewidth is 200 kc/sec. The vapor temperature is approximately 1000°C.